Title: Role of phosphorylated Smad3 signal components in intraductal papillary mucinous neoplasm of pancreas

Author: Yuichi Hori[1], Tsukasa Ikeura[1], Takashi Yamaguchi[1], Katsunori Yoshida[1], Koichi Matsuzaki[1], Mitsuaki Ishida[2], Sohei Satoi[3], Kazuichi Okazaki[1, *]

Author abbreviations: Hori Y, Ikeura T, Yamaguchi T, Yoshida K, Matsuzaki K, Ishida M, Satoi S, Okazaki K

City: *Osaka, Japan*

Author Affiliations:

1. Department of Gastroenterology and Hepatology, Kansai Medical University, 2-5-1 Shinmachi, Hirakata, Osaka 5731191, Japan

2. Department of Pathology, Kansai Medical University, 2-5-1 Shinmachi, Hirakata, Osaka 5731191, Japan

3. Department of Surgery, Kansai Medical University, 2-5-1 Shinmachi, Hirakata, Osaka 5731191, Japan

*Corresponding Author: Kazuichi Okazaki (Email: okazaki@hirakata.kmu.ac.jp)

ABSTRACT

Background: Malignant intraductal papillary mucinous neoplasm (IPMN) has poor prognosis. The carcinogenesis of IPMN is not clear. The aim of this study was to clarify transitions in phosphorylated Smad3 signaling during IPMN carcinogenesis.

Methods: By using immunohistochemistry, we examined the expression of pSmad3C and pSmad3L from 51 IPMN surgical specimens resected at our institution between 2010 and 2013. We also examined the expression of Ki-67, c-Myc and p-JNK .

Results: The median immunostaining index of pSmad3C was 79.2% in low-grade dysplasia, 74.9% in high-grade dysplasia, and 42.0% in invasive carcinoma (P <0.01), whereas that of pSmad3L was 3.4%, 4.3%, and 42.4%, respectively (P <0.01). There was a negative relationship between the expression of pSmad3C and c-Myc (P<0.001, r = -0.615) and a positive relationship between the expression of pSmad3L and c-Myc (P<0.001, r = 0.696). Negative relationship between the

expression of pSmad3C and Ki-67 ($P<0.01$, r = -0.610) and positive relationship between the expression of pSmad3L and Ki-67 ($P<0.01$, r = 0.731) were confirmed. p-JNK-positive cells were frequently observed among pSmad3L-positive cancer cells. The median of pSmad3L/pSmad3C ratio in the non-recurrence group and the recurrence group were 0.58 (range, 0.05-0.93), 3.83 (range, 0.85-5.96), respectively (P = 0.02). The median immunostaining index of c-Myc in the non-recurrence group and the recurrence group were 2.91 (range, 0-36.9) and 82.1 (range, 46.2-97.1), respectively (P=0.02). The median immunostaining index of Ki-67 in the non-recurrence group and the recurrence group were 12.9 (range 5.69-30.8) and 90.9 (range 52.9-98.5), respectively (P = 0.02).

Conclusions: pSmad3L was upregulated in malignant IPMN. pSmad3L/pSmad3C ratio may be a useful prognostic factor in IPMN.

Keywords: Intraductal papillary mucinous neoplasms of the pancreas; Immunohistochemistry; Phosphorylated Smad; Carcinogenesis; Prognosis

Introduction

Intraductal papillary mucinous neoplasm (IPMN) of the pancreas is the precursor lesion of pancreatic cancer, characterized by intraductal papillary growth and mucin secretion [1,2]. Unlike pancreatic ductal adenocarcinoma (PDAC), which

is characterized by a progressive pattern from pancreatic intraepithelial neoplasia (PanIN) to invasive ductal carcinoma [1], the IPMN carcinogenesis proceeds in an adenoma-carcinoma sequence that evolves from adenoma (low-grade dysplasia) to non-invasive cancer (high-grade dysplasia), and eventually to invasive cancer (invasive carcinoma) [3,4]. IPMN is a slowly growing cancer; however, once it progresses to invasive carcinoma, the prognosis is poor, and the five-year survival is approximately 40%-60% [5]. Therefore, in clinical practice, it is important to make an accurate decision on the timing of surgical resection for high-grade dysplasia and invasive carcinoma and to avoid excessive and unnecessary surgery for low-grade dysplasia.

Transforming growth factor beta (TGF-β) is a multifunctional cytokine that regulates cell growth and differentiation, matrix production, and apoptosis. The TGF-β signal is transmitted mainly through Smads, although a non-Smad transmission pathway is also known. Initially, TGF-β binds to the type II receptor on cell membrane and recruits the type I receptor (TβRI). The activated TβRI catalytically phosphorylates the COOH-terminal serine residues of receptor-activated Smads (R-Smads), such as Smad2 and Smad3 [6]. The Smad protein is composed of Mad homology 1 (MH1), the intermediate linker, and Mad homology 2 (MH2) domains [7]. The linker domain of Smad3 is phosphorylated by the mitogen-activated

protein kinase (MAPK) family members, including c-Jun NH2-terminal kinase (JNK)

[7-11]. Thus, TβRI and JNK phosphorylate Smad3 in a different pathway. Three types

of phospho-isoforms of Smad3 have been identified, namely COOH-terminally

phosphorylated Smad3 (pSmad3C), linker-phosphorylated Smad3 (pSmad3L), and

Smad3 phosphorylated at both the sites (pSmad3L/C). The phosphorylated Smad3

binds to Smad4, and is then translocated to the nucleus, where it regulates the

expression of target genes, both by direct DNA binding and through interaction with

other transcription factors, coactivators, and corepressors [7,9].

Smad-dependent signaling results in biphasic function through two distinct

pathways: a cytostatic TGF-β signal is transduced via pSmad3C and a

pro-tumorigenic TGF-β signal is transduced via pSmad3L (Fig. 1). In normal

epithelial cells, TGF-β-mediated pSmad3C signaling represents a major growth

inhibitory signal [12]. In cancer cells, on the other hand, JNK-mediated pSmad3L

signaling interferes with pSmad3C signaling and promotes tumor development and

growth by upregulation of c-Myc expression [7,9,12]. Although activated JNK

induces the transition from a tumor-suppressive pSmad3C pathway to an oncogenic

pSmad3L pathway during liver and colorectal carcinogenesis in humans [13], there

are no published studies on pSmad3 signaling in IPMN.

The aim of the present study was to test a hypothesis that transition from a

tumor-suppressive pSmad3C pathway to an oncogenic pSmad3L pathway occurs in

the progress of IPMN from low-grade to high-grade dysplasia, and eventually to

invasive carcinoma. Moreover, we also determined whether the assessment of

pSmad3C and pSmad3L in resected IPMN specimens would help in predicting the

postoperative prognosis of patients with malignant IPMN.

Methods

Patients and tissues

This study was approved by the ethical committee of Kansai Medical

University (No.H151047).

A retrospective analysis of data from 51 post-operative patients with IPMN

registered in our institution from 2010 to 2013 was performed. Of the 51 patients, 38

underwent surgical resection because of presence of predictors for malignancy, such

as enhancing solid component within cyst, main pancreatic duct >10 mm in size, and

mural nodule, according to the international consensus guidelines for the management

of IPMN [14,15]. The remaining 13 patients without predictors for malignancy had

undergone surgical resection because of dilated main pancreatic duct (5-9 mm in

diameter) or enlarging size of cyst during follow-up. Samples of normal pancreas

were collected from the pancreatic tissue adjacent to the resected serous cyst

neoplasms for use as controls. The following clinicopathological characteristics of patients were assessed: sex, age at surgery, image findings (main pancreatic duct diameter, existence of mural nodule, cyst diameter), laboratory data (carcinoembryonic antigen value, carbohydrate antigen 19-9 value), prognosis after surgery, and histological findings of the resected specimen.

Histological analysis

IPMNs were histologically categorized into IPMN with low-grade dysplasia, IPMN with high-grade dysplasia, and invasive carcinoma according to the World Health Organization Classification of Tumors of the Digestive System [16].

Domain-specific antibodies against phosphorylated Smad3

Two polyclonal anti-phospho-Smad3 sera, namely pSmad3L (Ser208/213) and pSmad3C (Ser423/425), were raised against the phosphorylated linker and COOH-terminal regions of Smad3 by immunizing rabbits with synthetic peptides. The antisera were affinity-purified using phosphorylated peptides as described below: one antiserum to the phosphorylated linker region of Smad3 (α pSmad3L [Ser 208/213]) was raised against the synthetic peptide (amino acids 200-215), in which serine residues at positions 208 and 213 were phosphorylated. Another antiserum to the phosphorylated C-terminal region of Smad3 [α pSmad3C (Ser 423/425)] was raised against the synthetic peptide (amino acids 416-425), in which serine residues at

positions 423 and 425 were phosphorylated. We previously confirmed that anti-pSmad3L antibody (Ab) and anti-pSmad3C Ab selectively recognized the phosphorylated linker region and phosphorylated C-terminal region, respectively [11].

Immunohistochemistry

Immunohistochemical analysis using the two polyclonal anti-phospho-Smad3 sera described above was performed as described previously [17]. Tissues were fixed by formalin within 3 h of resection, then fixed with 10% formalin solution for 24 h. Briefly, formalin-fixed and paraffin-embedded specimens were prepared, and 3-μm thick sections were cut. The sections were deparaffinized and rehydrated using xylene and a graded descending series of alcohol before staining. Nonenzymatic antigen retrieval was performed by heating the sections to 121 °C in 0.01 mol/L sodium citrate buffer (pH 6.0) for 15 min. After cooling, the sections were rinsed in Tris-buffered saline containing 0.1% Tween 20 (TBST) and incubated in a mixture of methanol and 3% H_2O_2 for 30 minutes to quench the endogenous peroxidase activity. Subsequently, the slides were incubated overnight at room temperature with each Ab. Thereafter, the sections were rinsed in TBST, incubated with peroxidase-labeled polymer conjugated to goat anti-mouse or anti-rabbit immunoglobulin (DAKO) for 1 h at room temperature, and subsequently rinsed again in TBST. Finally, the sections were developed with 3,3′-diaminobenzidine tetrahydrochloride (Vector Laboratories,

Burlingame, CA), counterstained with hematoxylin (Merck, Darmstadt, Germany), and mounted under coverslips.

Primary antibodies used in this study included rabbit polyclonal anti-Smad3C (Ser 423/425 phosphorylated) Ab (0.5 μg/mL; Immuno-Biological Laboratories Co., Gunma, Japan), rabbit polyclonal anti-Smad3L (Ser 208/213 phosphorylated) Ab (2 μg/mL; Immuno-Biological Laboratories Co.), mouse monoclonal anti-c-Myc Ab (10 μg/mL; Santa Cruz Biotechnology, Santa Cruz, CA, USA), mouse monoclonal anti-Ki-67 Ab (0.8 μg/mL, DAKO, Glostrup, Denmark), anti-p-JNK Ab (G-7, 1:50; Santa Cruz Biotechnology.), and anti-Smad4 Ab (B-8, 1:100; Santa Cruz Biotechnology). The affinity-purified rabbit polyclonal anti-pSmad3L (2 μg/mL) and anti-pSmad3C (0.5 μg/mL) Abs were described above.

Evaluation of immunostaining for pSmad3C, pSmad3L, and Ki-67

The cells that were immunoreactive for pSmad3C, pSmad3L, c-Myc, and Ki-67 in IPMN were counted in three randomly selected fields of view under high magnification (×400). The average percentage of immunoreactive cells in the three areas was defined as the immunostaining index.

Statistical analysis

All statistical analyses were carried out using JMP statistical software (version 13; SAS Institute, Cary, NC, USA) and the results were expressed as median and

range. Comparisons of categorical variables were conducted using the Fisher exact tests. Comparisons between the two groups and among the three groups were made using Mann–Whitney U test and Nonparametric Wilcoxon test, respectively. P values less than 0.05 were considered statistically significant.

Results

Clinicopathological features of patients with IPMN

The clinicopathological features of patients enrolled in the current study are shown in Table 1. Of the 51 patients, 28 (54.9%) were diagnosed with low-grade dysplasia, 8 (15.7%) with high-grade dysplasia, and 15 (29.4%) with invasive carcinoma derived from IPMN. Based on the morphological type, three (5.9%) patients were classified into the main duct type, 17 (33.3%) were classified into the mixed type, and 31 (60.8%) were classified into the branch duct type of IPMN. Of the 51 patients, 5 received postoperative chemotherapy. Five (9.8%) patients had recurrence of carcinoma, and the median time to recurrence was 6.8 months (range 6.0-32.8 months).

Immunohistochemistry for Smad4

Expression of Smad4 was immnohistochemically confirmed in all cases (images not shown).

Immunohistochemistry for pSmad3L and pSmad3C in normal pancreatic tissues and IPMNs

In the normal pancreatic tissue, pSmad3C was frequently detected in the nucleus of pancreatic duct epithelial cells, acinar cells, and islets cells (Fig. 2B), whereas few pSmad3L-positive cells were observed in the specimen (Fig. 2C). The images of immunohistochemical staining for pSmad3L and pSmad3C in low-grade dysplasia, high-grade dysplasia, and invasive carcinoma are also shown in Fig. 2. In IPMN with low-grade dysplasia, staining of pSmad3C was confirmed in the nucleus of numerous tumor cells (Fig.2E), whereas there were very few pSamd3L-positive tumor cells (Fig. 2F). In IPMN with high-grade dysplasia, less number of tumor cells were immunopositive for pSmad3C (Fig. 2H), whereas the immunopositivity of pSmad3L was increased compared to that in low-grade dysplasia (Fig. 2I). Furthermore, in invasive carcinoma, the expression of pSmad3C in tumor cells became much less (Fig. 2K), whereas that of pSmad3L was enhanced (Fig. 2L).

The median total number of cells in the immunohistochemically evaluated area was 223.5 (165.5-304.5). As IPMN progressed from low-grade dysplasia to high-grade dysplasia, and subsequently to invasive carcinoma, the median immunostaining index of pSmad3C was decreased (79.2% in low-grade dysplasia, 74.9% in high-grade dysplasia, and 42.0% in invasive carcinoma) (Fig. 3A).

Moreover, the median immunostaining index of pSmad3L increased with the progression of IPMN (3.4% in low-grade dysplasia, 4.3% in high-grade dysplasia, and 42.4% in invasive carcinoma) (Fig. 3B). There were statistically significant differences in the immunostaining index of pSmad3C and pSmad3L among low-grade dysplasia, high-grade dysplasia, and invasive carcinoma groups ($P<0.01$). The median of pSmad3L/pSmad3C ratio (the immunostaining index of pSmad3L divided by that of pSmad3C) in low-grade dysplasia, high-grade dysplasia, and invasive carcinoma were 0.04, 0.06, and 0.95, respectively, and the ratio significantly increased with the progression of IPMN ($P<0.01$, Fig. 3C).

Distributive association of pSmad3L and c-Myc in invasive carcinoma derived from IPMN

Because pSmad3L signaling accelerates tumor growth and invasion in concordance with the up-regulation of c-Myc, we investigated the relationship between the distribution of pSmad3L and c-Myc in invasive carcinoma. The nuclei of numerous carcinoma cells exhibited immunoreactivity for c-Myc. In an adjacent serial section, immunoreactivity for pSmad3L was observed in the nuclei of cells in the cancerous area showing c-Myc positivity (Fig. 4). Expression of c-Myc was rarely seen in low-grade dysplasia. The number of c-Myc positive cells increased in high-grade dysplasia, and c-Myc was more abundantly expressed in invasive

carcinoma compared to that in low- and high-grade dysplasia (Fig. 4A-C). There was

a significantly negative relationship between the expression of pSmad3C and c-Myc

(P<0.001, r = -0.615; Fig. 4D) and a significantly positive relationship between the

expression of pSmad3L and c-Myc (P<0.001, r = 0.696; Fig. 4E).

Correlative evaluation of immunostaining index between pSmad3C and Ki-67 and

between pSmad3L and Ki-67

The distribution of Ki-67-positive cells in IPMN is shown in Fig. 5.

Expression of Ki-67 was rarely seen in low-grade dysplasia (Fig. 5A, D). The number

of Ki-67-positive cells increased in high-grade dysplasia (Fig. 5B, E), and Ki-67 was

more abundantly expressed in invasive carcinoma compared to that in low- and

high-grade dysplasia (Fig. 5C, F). There was a significant negative relationship

between the expression of pSmad3C and Ki-67 (P<0.01, r = -0.610) and a significant

positive relationship between the expression of pSmad3L and Ki-67 (P<0.01, r =

0.731; Fig. 5G, H).

Distributive association of pSmad3L and phosphorylated JNK (p-JNK) in invasive

carcinoma

To investigate the upstream signal of pSmad3L, distributive association of

pSmad3L and p-JNK was immunohistochemically evaluated. Significant expression

of p-JNK was observed in the cytoplasm and nuclei of invasive carcinoma, and

significant expression of pSmad3L is expressed in the nucleus in an adjacent serial section (Fig. 6).

Comparison of pSmad3 signaling between the recurrence group and the non-recurrence group of IPMN with high-grade dysplasia/invasive carcinoma

To study the correlation between signal alteration of pSmad3 and recurrence of carcinoma, patients with high-grade dysplasia and invasive carcinoma were divided into two groups, namely recurrence group (n = 5) and non-recurrence group (n = 18). The pSmad3L/pSmad3C ratio between the two groups was compared. The median follow-up period of 23 patients with high-grade dysplasia and invasive carcinoma was 62 (38-75) days. The median of pSmad3L/pSmad3C ratio in the non-recurrence group and the recurrence group were 0.58 (range, 0.05-0.93), 3.83 (range, 0.85-5.96) respectively (P = 0.02, Fig. 7). We also compared the immunostaining index of Ki-67 and that of c-Myc between the recurrence group and the non-recurrence group. The median immunostaining index of c-Myc in the non-recurrence group and the recurrence group were 2.91 (range, 0-36.9) and 82.1 (range, 46.2-97.1), respectively (P=0.02). The median immunostaining index of Ki-67 in the non-recurrence group and the recurrence group were 12.9 (range 5.69-30.8) and 90.9 (range 52.9-98.5), respectively (P = 0.02).

Discussion

The carcinogenesis of IPMN results from the accumulation of various molecular genetic abnormalities. An understanding of the molecular mechanisms can lead to the development of biomarkers for early detection of the cancer and devising of treatment strategies using agents for molecular targets. In the present study, a marked expression of cancer-related c-Myc was observed in pSmad3L-positive cells in invasive carcinoma, while pSmad3L and c-Myc-positive cells were less often seen in low-grade and high-grade dysplasia. Moreover, the expression of pSmad3L and Ki-67 exhibited a positive correlation. Similar to the previous studies on oncogenic process in liver and colorectal cancer [13], these results suggest that pSmad3L can promote the proliferation of tumor cells through c-Myc in IPMN.

Tumorigenic growth appears to be essentially a cell-autonomous phenomenon that involves a shift from the tumor-suppressive pSmad3C pathway to the oncogenic pSmad3L pathway induced by alterations in the genome of cancer cells, such as in the Ras oncogene [12]. Previously, Sekimoto et al. demonstrated that Ras-activated JNK/pSmad3L signaling was able to provide oncogenic potential to the epithelial cells by up-regulation of c-Myc, resulting in strongly enhanced tumor growth and invasion [18]. In IPMN, mutation of Kras, the most frequently mutated Ras gene, was observed in 56%–81% of the cases, and its frequency was reported to increase with the

progression of tumor [16,19,20]. Therefore, Kras-induced JNK/pSmad3L signaling may be one of the promoters of IPMN carcinogenesis.

The oncogenic pSmad3L signal and the tumor-suppressive pSmad3C signal have opposite functions. When phosphorylation of the linker region of Smad3 is specifically blocked by inhibiting JNK activation or by substituting the phosphorylation site of the linker region with an unphosphorylated amino acid, the pSmad signaling reverts from the oncogenic pSmad3L pathway to the tumor-suppressive pSmad3C pathway [12,21]. The reversibility from pSmad3L to pSmad3C pathway has been demonstrated not only in cultured cells, but also in animal experiments. As a result of administration of a JNK inhibitor to rats, hepatic carcinogenesis was significantly suppressed. In that case, alteration from the oncogenic pSmad3L/c-Myc signaling pathway to tumor-suppressive pSmad3C/p21^{WAF1} signaling pathway was observed in hepatocytes of rat liver tissue upon administration of a JNK inhibitor. These results theoretically support the molecular target therapy of cancer. Considering the results obtained in the present study, biomolecular therapy targeting the JNK/pSmad3L signaling might offer an effective treatment for carcinoma derived from IPMN.

Currently, the Fukuoka criteria for the management of IPMN have been widely accepted. Although its sensitivity for prediction of high-grade dysplasia and invasive

carcinoma in branch duct IPMN appears to be relatively high, the specificity still remains unsatisfactory [22]. Based on the results of the present study, preoperative molecular analysis of pSmad3C and pSmad3L in pancreatic juice obtained through endoscopic retrograde cholangiopancreatography (ERCP) or cystic fluid obtained using endoscopic ultrasound-guided fine needle aspiration (EUS-FNA) may provide additional information on decision for surgery to improve the accuracy of the Fukuoka criteria.

Regarding Smad3 phosphorylation for predicting the risk of HCC, chronic hepatitis HBV/HCV patients, with high levels of pSmad3L and low pSmad3C in liver tissues, had a higher risk of developing HCC than those with low pSmad3L expression and high pSmad3C expression [23]. Thus, the grading of hepatocytic pSmad3C/3L levels in HBV/HCV-inflected livers has been shown to be a clinically useful biomarker for predicting the risk of later development of HCC. In the present study, it has been demonstrated that the pSmad3L/pSmad3C ratio in the recurrence group was significantly higher than that in the non-recurrence group in resected pancreas in patients with high-grade dysplasia IPMN and invasive carcinoma. Regarding Ki-67 and c-Myc as well, significant differences were observed between the recurrence groups and non-recurrence group. These results are considered reasonable because c-Myc and Ki-67 are downstream signals of pSmad3L. These data

suggest that the immunohistochemical evaluation of pSmad3L and pSmad3C may be a potentially useful biomarker for prediction of postoperative recurrence in the patients with high-grade dysplasia and invasive carcinoma.

In conclusion, the present study reveals that phosphorylated Smad3 signaling in the pancreas of patients with IPMN is converted from pSmad3C signaling to pSmad3L signaling as the tumor progresses during the oncogenic process, suggesting that such a signal alteration of pSmad3 might contribute to carcinogenesis in IPMN. In addition, the pSmad3L/pSmad3C ratio in post-operative patients with high-grade dysplasia and invasive carcinoma may be a novel biomarker for predicting the recurrence. Further large-scale study may be needed to offer more reliable evidence on prediction of carcinogenesis and prognosis in IPMN by focusing on intracellular signaling alteration of pSmad3.

References

1   Tanaka M, Fernández-Del Castillo C, Kamisawa T, Jang JY, Levy P, Ohtsuka T, et al. Revisions of international consensus Fukuoka guidelines for the management of IPMN of the pancreas. Pancreatology 2017;17:738-753.

2   Bosman FT, International Agency for Research on C. WHO classification of tumours of the digestive system, 4th ed: International Agency for Research on

Cancer; 2010.

3   Fritz S, Fernandez-del Castillo C, Mino-Kenudson M, Crippa S, Deshpande V,

Lauwers GY, et al. Global genomic analysis of intraductal papillary mucinous

neoplasms of the pancreas reveals significant molecular differences compared to

ductal adenocarcinoma. Ann Surg 2009;249:440-447.

4   Distler M, Aust D, Weitz J, Pilarsky C, Grützmann R. Precursor lesions for

sporadic pancreatic cancer: PanIN, IPMN, and MCN. Biomed Res Int

2014;2014:474905.

5   Grützmann R, Niedergethmann M, Pilarsky C, Klöppel G, Saeger HD.

Intraductal papillary mucinous tumors of the pancreas: Biology, diagnosis, and

treatment. Oncologist 2010;15:1294-1309.

6   Wrana JL. Crossing Smads. Sci STKE 2000;2000:re1.

7   Yamaguchi T, Yoshida K, Murata M, Matsuzaki K. Smad3 phospho-isoform

signaling in hepatitis C virus-related chronic liver diseases. World J

Gastroenterol 2014;20:12381-12390.

8   Murata M, Matsuzaki K, Yoshida K, Sekimoto G, Tahashi Y, Mori S, et al.

Hepatitis B virus X protein shifts human hepatic transforming growth factor

(TGF)-beta signaling from tumor suppression to oncogenesis in early chronic

hepatitis B. Hepatology 2009;49:1203-1217.

9   Yoshida K, Matsuzaki K, Murata M, Yamaguchi T, Suwa K, Okazaki K. Clinico-pathological importance of TGF-β/phospho-smad signaling during human hepatic fibrocarcinogenesis. Cancers (Basel) 2018;10:183.

10   Mori S, Matsuzaki K, Yoshida K, Furukawa F, Tahashi Y, Yamagata H, et al. TGF-beta and HGF transmit the signals through JNK-dependent Smad2/3 phosphorylation at the linker regions. Oncogene 2004;23:7416-7429.

11   Furukawa F, Matsuzaki K, Mori S, Tahashi Y, Yoshida K, Sugano Y, et al. p38 MAPK mediates fibrogenic signal through Smad3 phosphorylation in rat myofibroblasts. Hepatology 2003;38:879-889.

12   Matsuzaki K. Smad phosphoisoform signaling specificity: The right place at the right time. Carcinogenesis 2011;32:1578-1588.

13   Yamagata H, Matsuzaki K, Mori S, Yoshida K, Tahashi Y, Furukawa F, et al. Acceleration of Smad2 and Smad3 phosphorylation via c-Jun NH(2)-terminal kinase during human colorectal carcinogenesis. Cancer Res 2005;65:157-165.

14   Tanaka M, Chari S, Adsay V, Fernandez-del Castillo C, Falconi M, Shimizu M, et al. International consensus guidelines for management of intraductal papillary mucinous neoplasms and mucinous cystic neoplasms of the pancreas. Pancreatology 2006;6:17-32.

15   Tanaka M, Fernández-del Castillo C, Adsay V, Chari S, Falconi M, Jang JY, et al.

International consensus guidelines 2012 for the management of IPMN and MCN of the pancreas. Pancreatology 2012;12:183-197.

16 Patra KC, Bardeesy N, Mizukami Y. Diversity of precursor lesions for pancreatic cancer: The genetics and biology of intraductal papillary mucinous neoplasm. Clin Transl Gastroenterol 2017;8:e86.

17 Yoshida K, Matsuzaki K, Mori S, Tahashi Y, Yamagata H, Furukawa F, et al. Transforming growth factor-beta and platelet-derived growth factor signal via c-Jun N-terminal kinase-dependent Smad2/3 phosphorylation in rat hepatic stellate cells after acute liver injury. Am J Pathol 2005;166:1029-1039.

18 Sekimoto G, Matsuzaki K, Yoshida K, Mori S, Murata M, Seki T, et al. Reversible Smad-dependent signaling between tumor suppression and oncogenesis. Cancer Res 2007;67:5090-5096.

19 Kuboki Y, Shimizu K, Hatori T, Yamamoto M, Shibata N, Shiratori K, et al. Molecular biomarkers for progression of intraductal papillary mucinous neoplasm of the pancreas. Pancreas 2015;44:227-235.

20 Wu J, Matthaei H, Maitra A, Dal Molin M, Wood LD, Eshleman JR, et al. Recurrent GNAS mutations define an unexpected pathway for pancreatic cyst development. Sci Transl Med 2011;3:92ra66.

21 Nagata H, Hatano E, Tada M, Murata M, Kitamura K, Asechi H, et al. Inhibition

of c-Jun NH2-terminal kinase switches Smad3 signaling from oncogenesis to tumor-suppression in rat hepatocellular carcinoma. Hepatology 2009;49:1944-1953.

22 Heckler M, Michalski CW, Schaefle S, Kaiser J, Büchler MW, Hackert T. The Sendai and Fukuoka consensus criteria for the management of branch duct IPMN - A meta-analysis on their accuracy. Pancreatology 2017;17:255-262.

23 Matsuzaki K, Murata M, Yoshida K, Sekimoto G, Uemura Y, Sakaida N, et al. Chronic inflammation associated with hepatitis C virus infection perturbs hepatic transforming growth factor beta signaling, promoting cirrhosis and hepatocellular carcinoma. Hepatology 2007;46:48-57.

Table 1. Demographics of patients in the present study (*n*=51)

Characteristics	Values
Age (yr)	70 (62-76)
Male	31 (60.8%)
CEA (ng/mL)	2.8 (1.9-4)
CA19-9 (U/mL)	11.9 (6.8-27.5)
Preoperative imaging findings	
Tumor size (cm)	27 (18-40)
Mural nodule	28 (54.9%)
MPD diameter (mm)	3.5 (2-7)
Preoperative evaluation according to Fukuoka Criteria	
Worrisome features	34 (66.7%)
High-risk stigmata	8 (15.7%)
Fulfilment of indication for resection according to Fukuoka criteria	
Yes	38 (74.5%)
No	13 (25.5%)
Morphological type	
Main	3 (5.9%)
Mixed	17 (33.3%)
Branch	31 (60.8%)
Pathological findings	
Low-grade dysplasia	28 (54.9%)
High-grade dysplasia	8 (15.7%)
Invasive carcinoma	15 (29.4%)
Stage [a]	
0	8 (34.8%)
I	5 (21.7%)
II	2 (8.7%)
III	4 (17.4%)
IV	4 (17.4%)
Recurrence	5 (21.7%)

[a] UICC classification. MPD:

Figure legends
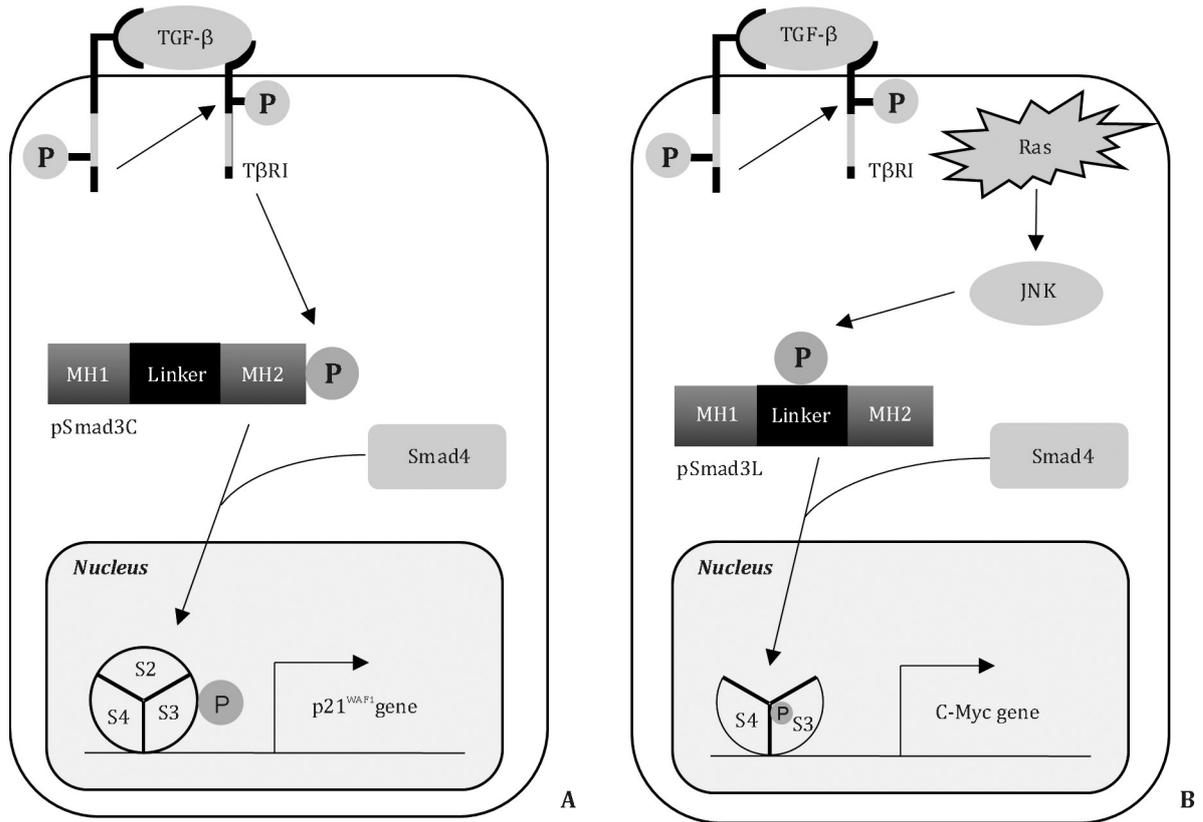
Fig. 1. The pathways of phosphorylated Smad3 signals in tumors. **A**: pSmad3C suppresses the cell growth via activation of p21^{WAF1} gene; **B**: pSmad3L stimulates tumor proliferation via activation of c-Myc gene. TGF-β: transforming growth factor beta; TβRI: TGF-β type I receptor; MH1: mad homology 1; MH2: mad homology 2; Linker: linker lesion; JNK: c-Jun NH2-terminal kinase.
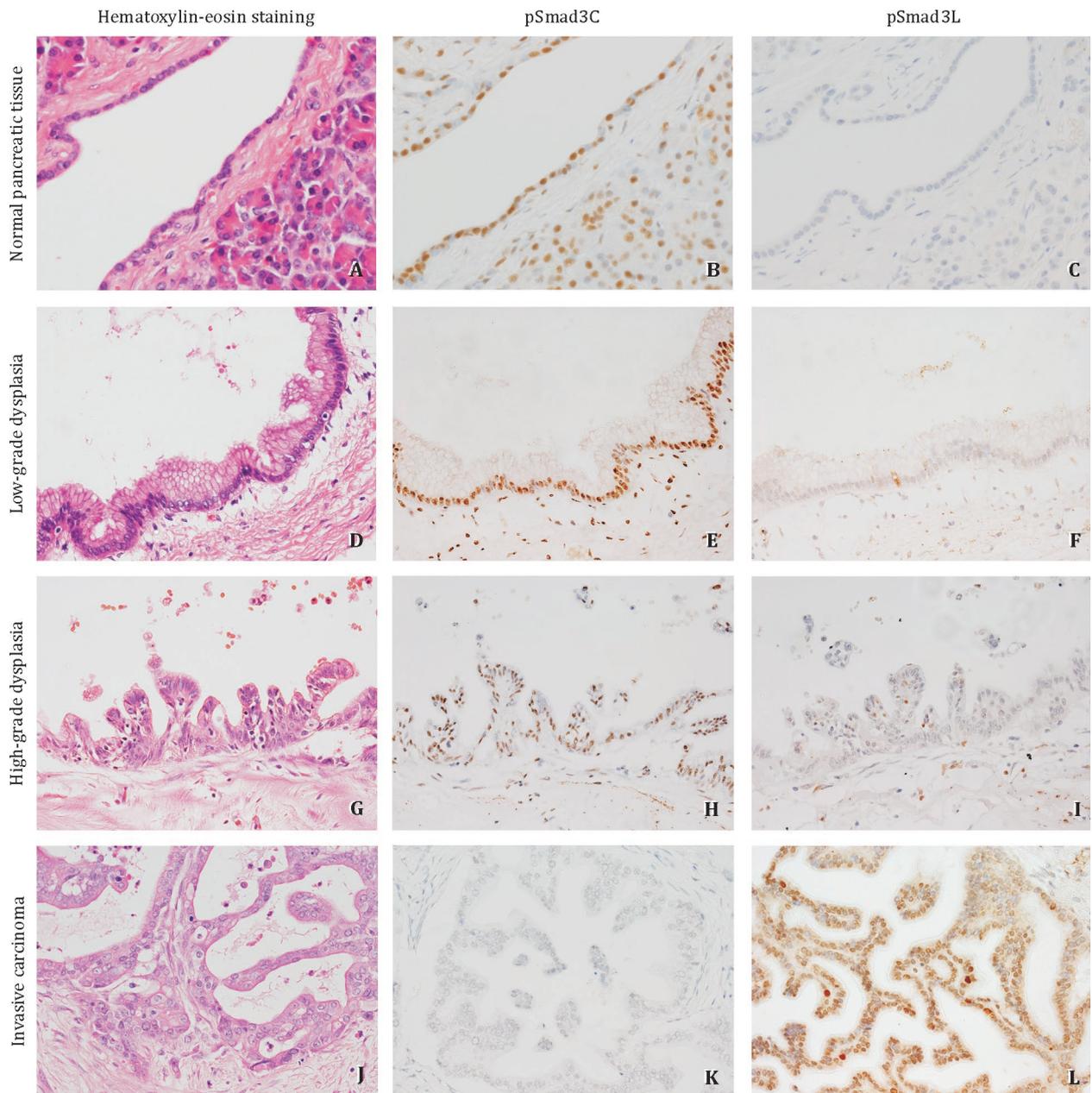
Fig. 2. Immunohistochemical staining of pSmad3L and pSmad3C in normal pancreatic tissue, IPMN with low- and high-grade dysplasia and invasive carcinoma. pSmad3C positive cells were gradually decreased following normal to invasive carcinoma transformation; pSmad3L positive cells were gradually increased following normal to invasive carcinoma transformation (original magnification ×400).
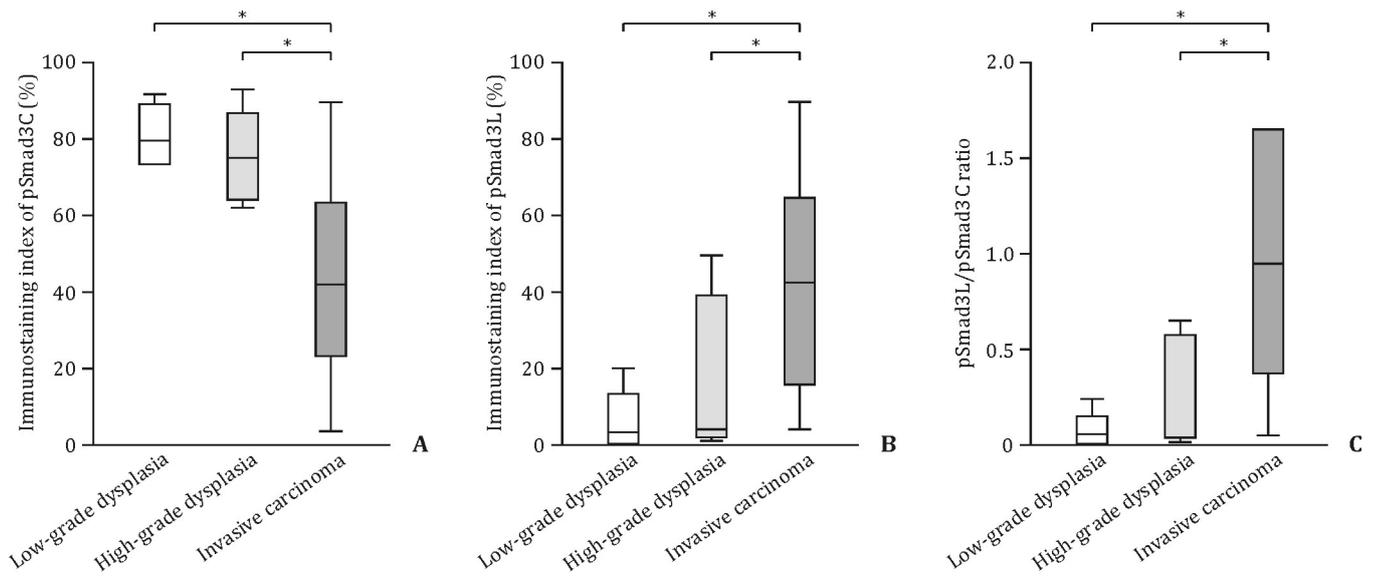
Fig. 3. Comparison of immunostaining index of pSmad3C and pSmad3L among low-

and high-grade dysplasia, and invasive carcinoma. *: *P*<0.01.
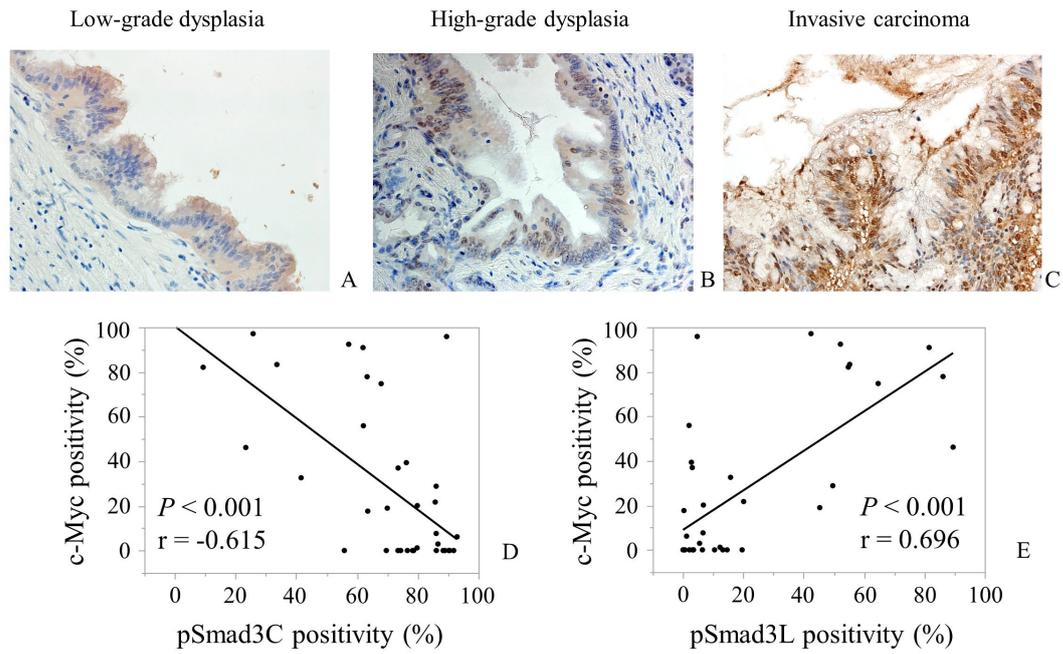
Fig. 4. c-Myc expression in different malignant grades (original magnification×400, **A-C**). There was a significantly negative relationship between the expression of pSmad3C and c-Myc (**D**) and a significantly positive relationship between the expression of pSmad3L and c-Myc (**E**).
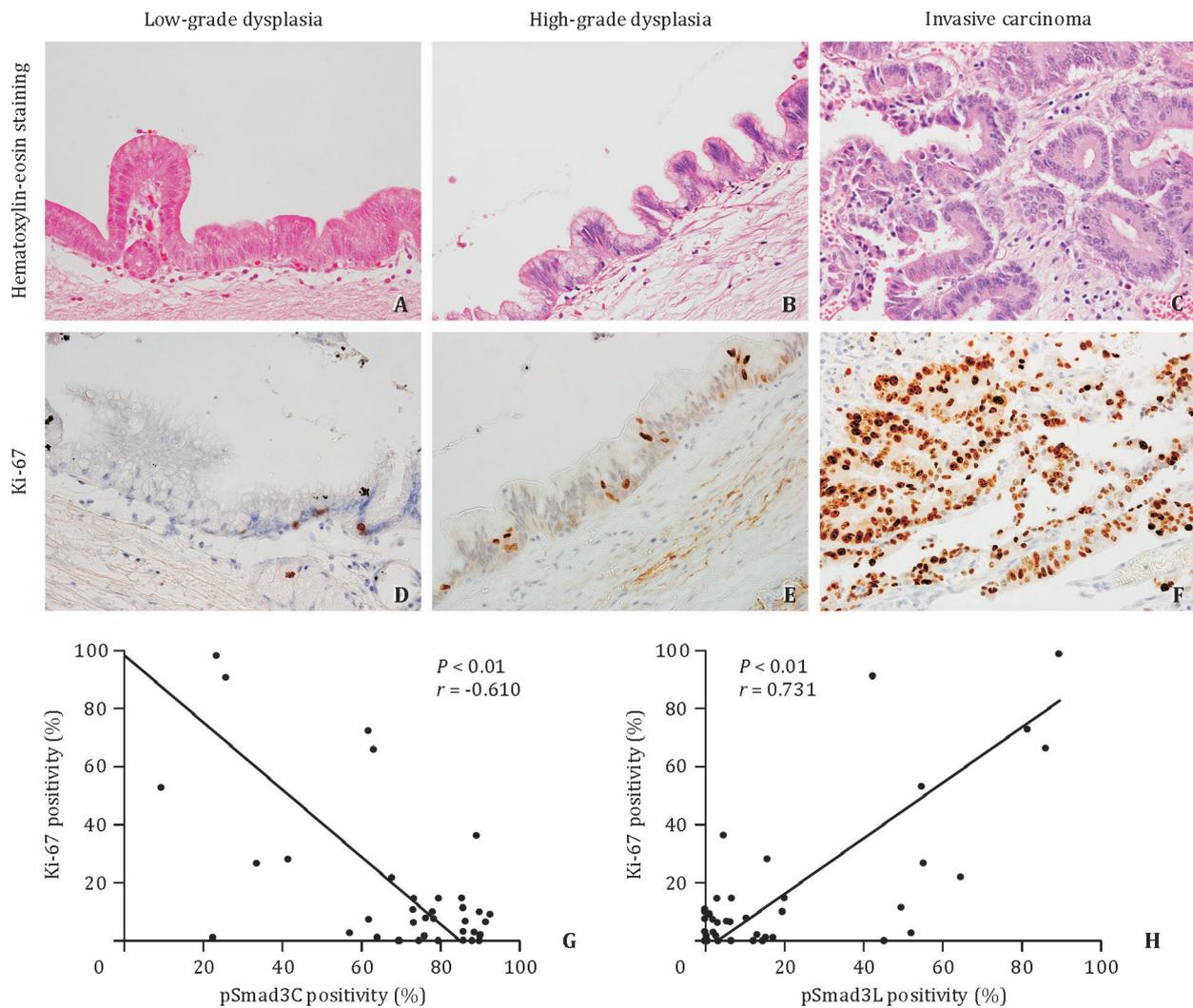
Fig. 5. Ki-67 staining and its correlation to phosphorylated Smad3.

Hematoxylin and eosin staining of IPMN in different malignant grades (original magnification×400, **A-C**). HE staining pictures and Ki-67 staining pictures are serial sections. Ki-67-positive cells were increased as IPMN progressed from low-grade dysplasia, to high-grade dysplasia and subsequently to invasive carcinoma (Original magnification×400, **D-F**). A significant negative relationship between the presence of pSmad3C and Ki-67 (**G**) and a significant positive relationship between the presence of pSmad3L and Ki-67 were observed (**H**).
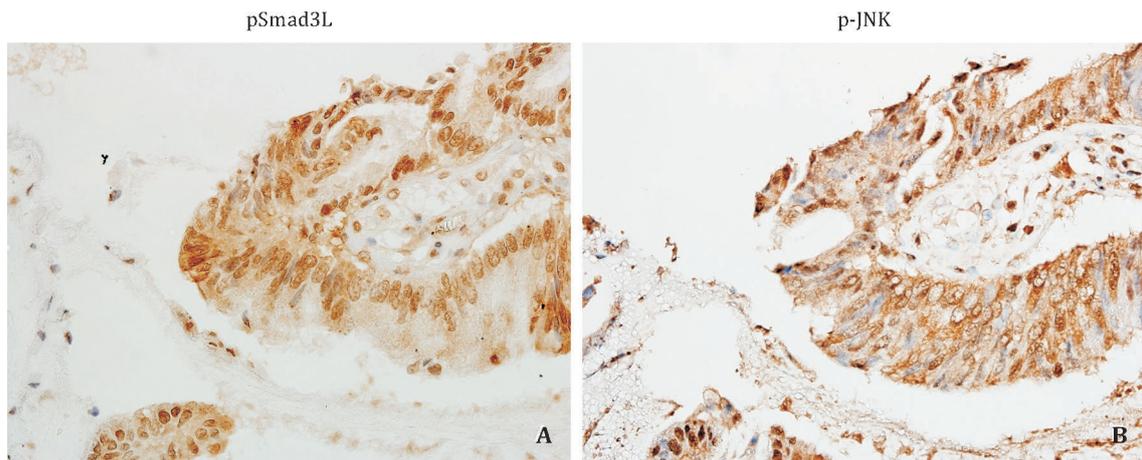
pSmad3L   p-JNK

Fig. 6. Immunostaining of pSmad3L and p-JNK in cell nuclei and cytoplasm of invasive carcinoma (original magnification×400). **A**: Significant expression of pSmad3L is expressed in the nucleus of invasive carcinoma; **B**: In an adjacent serial section, significant expression of p-JNK was observed in the cytoplasm and nuclei.
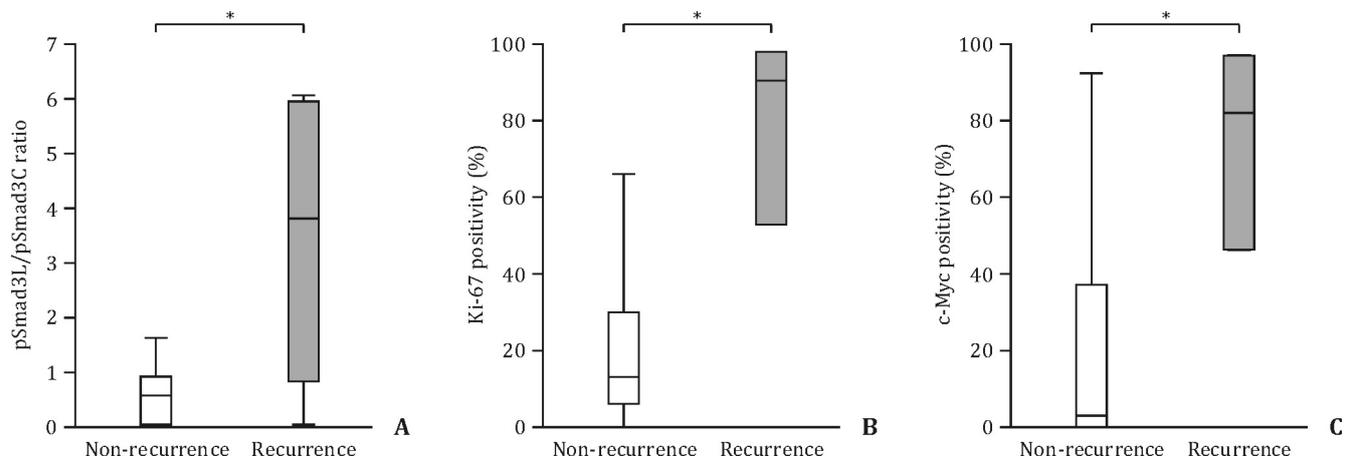
Fig. 7. Comparison of pSmad3L/pSmad3C immunostaining positivity ratio, immunostaining index of Ki-67 and c-Myc in the tumor cells between in the recurrence group and the non-recurrence group of IPMN with high-grade dysplasia/invasive carcinoma. **A**: pSmad3L/pSmad3C ratio in the recurrence group is shown to be significantly higher than that in the non-recurrence group; **B**: There was a significant difference in immunostaining index of Ki-67 between the recurrence group and the non-recurrence group; **C**: In immunostaining index of c-Myc, a significant difference was observed between the recurrence group and the non-recurrence group. *: *P*<0.05.